J Mater Sci (2020) 55:2764–2771

Ceramics

$Ba_{0.1}Sr_{0.9}Zr_{0.18}Ti_{0.82}O_3$ ceramics: dielectric properties and energy storage density under external electric field and temperature

Tao Zhang[1], Haibibu Aziguli[1], Yanhong Wu[1], Jie Yin[1], and Ping Yu[1,*]

[1] *Department of Materials Science, Sichuan University, Chengdu 610064, People's Republic of China*

Received: 19 September 2019
Accepted: 22 November 2019
Published online: 1 December 2019

ABSTRACT

In order to develop the application of energy storage ceramics, the dielectric properties and energy storage density of $Ba_{0.1}Sr_{0.9}Zr_{0.18}Ti_{0.82}O_3$ ceramics (BSZT-118) prepared by the modified sol–gel process were researched under different temperatures under electric field. The results show that the dielectric constant of BSZT-118 is consistent with Johnson's formula based on Devonshire phenomenological theory, and the anharmonic constant (α) increases as the temperature rises. The energy storage density of BSZT-118 is influenced by the electric field and temperature. With the increase in temperature, the storage density of BSZT decreases and the fluctuation of storage density increases under electric field. The conduction mechanism of BSZT-118 is mainly space charge-limited conduction (SCLC) below 60 °C, and it is mainly Ohmic conduction above 60 °C.

Introduction

The high-energy density pulse capacitors are applied for electromagnetic weapon, medical defibrillators and other applications because of the increasingly deteriorated energy crisis [1–3]. Simultaneously, there is a great challenge for pulse capacitors to have larger energy density, less loss and better stability [4–6]. The barium titanate (BT) researched by many researchers is commonly used as the major component in ceramic capacitor dielectrics [7–9]. Furthermore, doping Sr can improve the room temperature dielectric constant through lowering the Curie temperature, and doping Zr has higher chemical stability as well as lower dielectric loss [10, 11]. In addition, Ricketts et al. [12] pointed that the stored dielectric energy density would reach 4 J/cm^3 for $Ba_{1-x}Sr_xZr_yTi_{1-y}O_3$ ceramics with $x > 0.7$ and $y \sim 0.2$ and Qing et al. [13] obtained the $Ba_{0.95}Sr_{0.05}Zr_{0.2}Ti_{0.8}O_3$ ceramic with storage density of 0.42 J/cm^3 by doping. The $Ba_{0.1}Sr_{0.9}Zr_{0.18}Ti_{0.82}O_3$ ceramics (BSZT-118) having high dielectric constant and low loss tangent have also been reported [14]. Based on the latest research, Mangaiyarkkarasi et al. [15] studied the precise electronic structure and bonding interactions of BSZT ceramics and Jian et al. [16] indicated that the BSZT ceramics change from a normal ferroelectric to

Address correspondence to E-mail: pingyu@scu.edu.cn

https://doi.org/10.1007/s10853-019-04248-3

a relaxor ferroelectric with increasing Zr^{4+} and Sr^{2+} ionic content.

However, the performance of the material is affected by the application environment. This work is to analyze the changes in dielectric properties and energy storage density of BSZT-118 under different external electric fields and temperatures, providing some basis for theoretical research on the use of energy storage capacitors, which is very important for the application of ceramic capacitors.

Experiment

BSZT-118 powders were prepared by the modified sol–gel process, i.e., polyacrylamide-gel method. Firstly, stoichiometric $Ba(CH_3COO)_2$, $Sr(NO_3)_2$ with $Zr(NO_3)_4{\cdot}5H_2O$ were dissolved in the deionized water with continuous stirring to get transparent aqueous solution. Then, stoichiometric $Ti(C_4H_9O)_4$ was added in a mixed solution of acetic acid and ethanol with acetylacetone as the stabilizer for getting the Ti source. Thirdly, the previous transparent aqueous solution mixed with Ti-containing solution with stirring 10 min in order to obtain a transparent sol. Next, N,N′-methylene-bis-acrylamide which was used as the cross-linking and acrylamide was dissolved into the sol with stirring for 1 h. Finally, azodiisobutyronitrile (AIBN) as the initiator was added into the as-prepared solution, which turned to hydrogel gradually when the solution was heated to 90 °C. After getting the dry gel, the xerogel was carbonized at 300 °C. Then, the xerogel after carbonization was calcined at 900 °C with urea as a sintering aid.

The as-prepared BSZT-118 powder was granulated using polyvinyl alcohol (PVA) as the binder and pressed into disks of 10 mm diameter with 1.0 mm thickness at 10 MPa using dry press forming. Next, the ceramic sheets were isostatic-pressed after excluding the binder. Then, the ceramic chips were sintered at 1300 °C. After that, the silver paste was sintered on both sides of the pellets at 700 °C for 10 min to form electrodes. Finally, the pellets were tested by different instruments.

Results and discussion

The typical XRD pattern of BSZT-118 shown in Fig. 1a was obtained by using the X-ray diffraction (XRD) (DX-1000, Dandong, China) in the range of diffraction angle 20°–90°, and it is cubic phase without impurity phase based on the diffraction pattern. The morphology of BSZT-118 was investigated using the HITACHI S4800 scanning electron microscope (SEM). As shown in Fig. 1b, BSZT-118 has high density and good micromorphology. In the meanwhile, the grain size of BSZT-118 is relatively uniform and the porosity is small.

Further research on the dielectric constant of BSZT-118 at different temperatures under the maximum electric field 100 kV/cm is necessary. In Fig. 2a, it is obvious that BSZT-118 is paraelectric phase from 20 to 120 °C and this result is consistent with the XRD pattern diffraction. Besides, the slope of the polarization hysteresis loop shown in Fig. 2a decreases as the temperature rises, which means that the dielectric constant declines and interpreted in Fig. 3.

In Fig. 2b, the dielectric constant decreases with the temperature from room temperature (20 °C) to 120 °C and with the increase in external electric field. The dielectric constant of the nonlinear relationship is weakening under external electric field with temperature from 20 °C to 120 °C. This mean that the higher the temperature, the weaker the dielectric constant is affected by the electric field, which may be because of thermal motion. According to the formula:

$$T = \frac{D_0}{D_0 - D_{100}} \times 100\% \quad (1)$$

where T is the rate of change and D_0 and D_{100} are dielectric constant at 0 kV/cm and 100 kV/cm, respectively. Based on calculation, from 20 to 120 °C, the rate of change of dielectric constant is from 17.3 to 11.2% when the electric field increases to 100 kV/cm in Fig. 2b.

In Fig. 3, according to the peak characteristics at the Curie point, the Curie temperature is lower than − 160 °C, which is consistent with previous reports [17, 18], and the dielectric constant reduces with increasing temperature above − 160 °C. Furthermore, the slope of the polarization hysteresis loop is positively related to the dielectric constant because BSZT-118 is the paraelectric phase from 20 to 120 °C. The formula is as follows

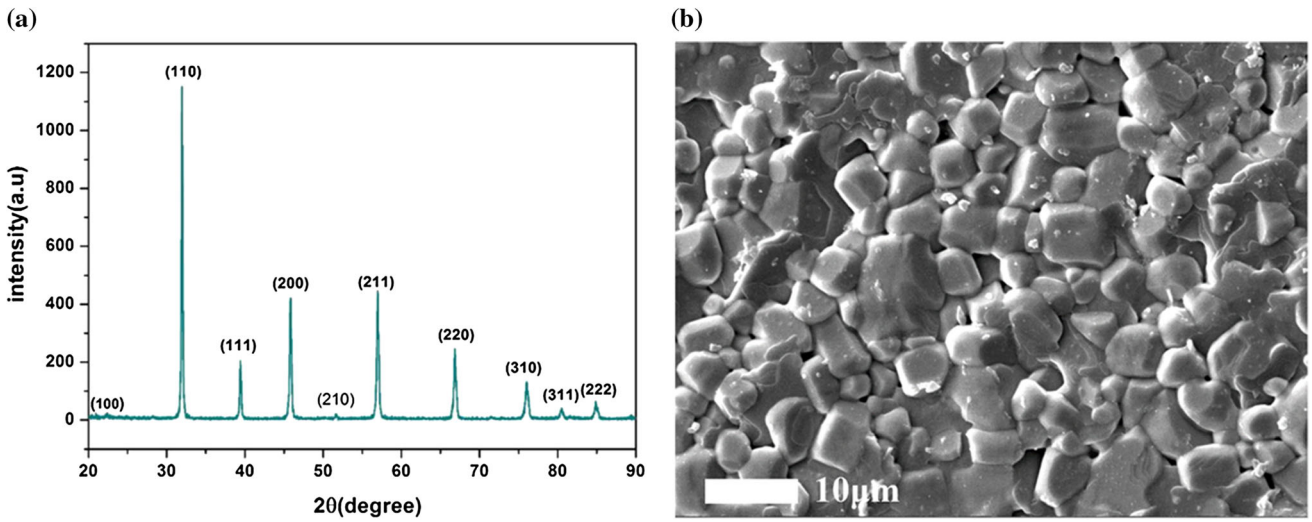

Figure 1 The XRD diffraction pattern of BSZT-118 (**a**) and the SEM image of BSZT-118 (**b**).

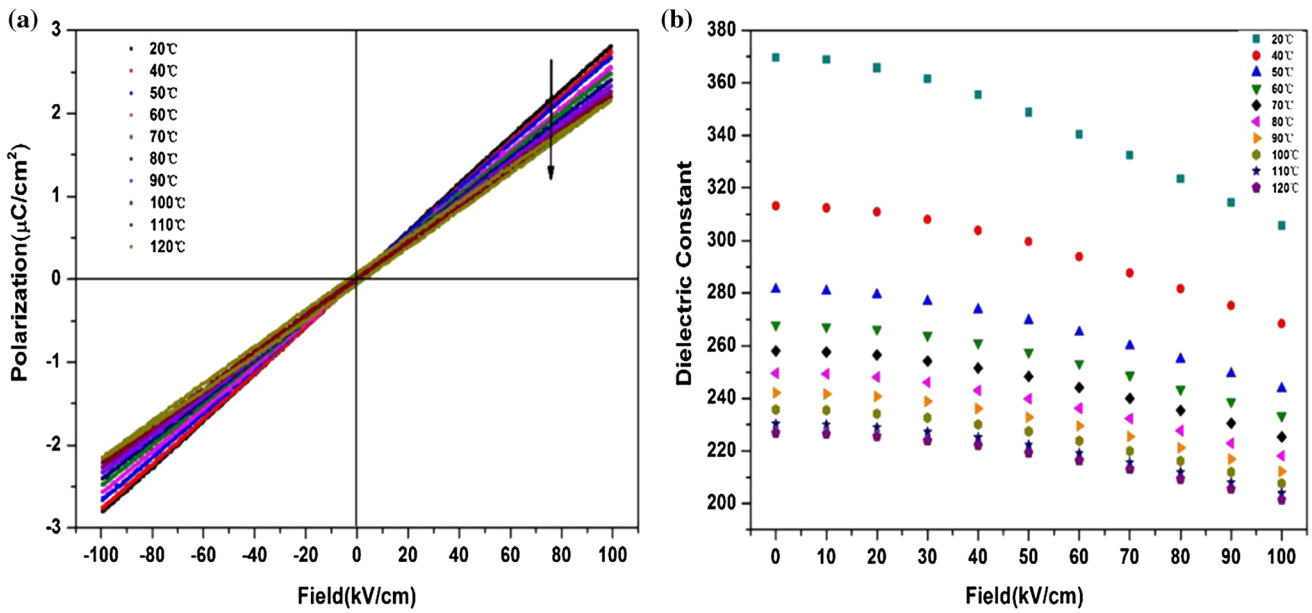

Figure 2 The polarization versus electric field hysteresis loops (**a**) and dielectric constant dependence of field strength (**b**) at different test temperatures.

$$dP = \varepsilon_0(\varepsilon_r - 1)dE \quad (2)$$

where P, ε_0, ε_r and E is the polarization intensity, vacuum dielectric constant, relative dielectric constant and applied electric field, respectively. Therefore, Fig. 3 explains why the slope of the polarization hysteresis loop decreases with the increase in temperature clearly. But the Curie temperature was not obtained because of limitation of the test conditions. Fig. 3 also shows that the curve becomes more smooth and stable from 20 to 120 °C that is consistent with the change rate of the permittivity in the above-mentioned results.

In addition, the dielectric constant of BSZT-118 is relative low because the test temperature (20–120 °C) is far from the Curie point and permittivity–temperature curve little affected by frequency has small peak about 0 °C, meanwhile, loss–temperature curve also has it, which might be caused by the phase change of water from the atmosphere (solid to liquid).

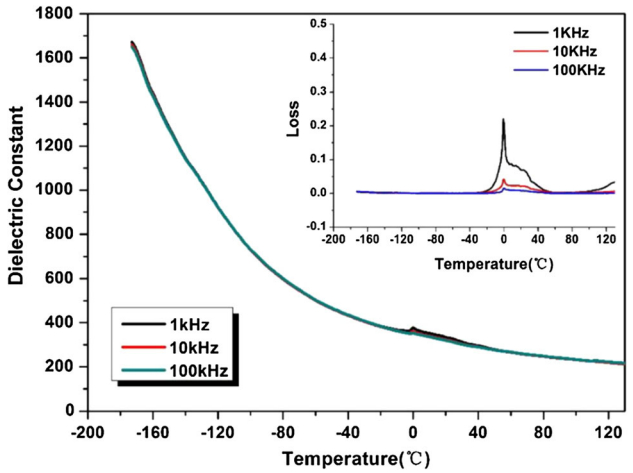

Figure 3 The dielectric properties dependence on the temperature for BSZT-118.

Researching the nonlinear dielectric response of BSZT-118, Johnson's formula is very important to describe the relationship between the dielectric constant and electric field quantitatively [19–21]. The formula is as follows:

$$\frac{\varepsilon(E)}{\varepsilon(0)} = \frac{1}{[1+\alpha\varepsilon^3(0)E^2]^{1/3}} \tag{3}$$

where $\varepsilon(E)$ and $\varepsilon(0)$ are the dielectric constant under external electric field and 0 kV/cm, respectively, and α is a positive constant associated with the anharmonic effect (here called anharmonic constant). This formula was derived by Johnson from the Devonshire phenomenological theory, as an approximation for the paraelectric phase when the Curie temperature is far from the test temperature.

To make it easier to observe the fit results, Johnson's formula deformed as:

$$\frac{\varepsilon(0)^3}{\varepsilon(E)^3} = 1 + \alpha\varepsilon^3(0)E^2 \tag{4}$$

It is showed that $\varepsilon(0)^3/\varepsilon(E)^3$ with E^2 is linear, and Fig. 4 shows good linear relationship between $\varepsilon(0)^3/\varepsilon(E)^3$ with E^2; this means that results of linear fit accorded with Johnson's formula, so BSZT-118 is suitable for Devonshire phenomenological theory and nonlinear dielectric behavior is mainly caused by the anharmonic interaction between Ti ion and Zr ion under high electric field [22, 23].

According to Fig. 4, there is anharmonic constant α obtained by above of linear fit at different test temperatures. The result shows that α increases as test temperature rises, which may be because anharmonic

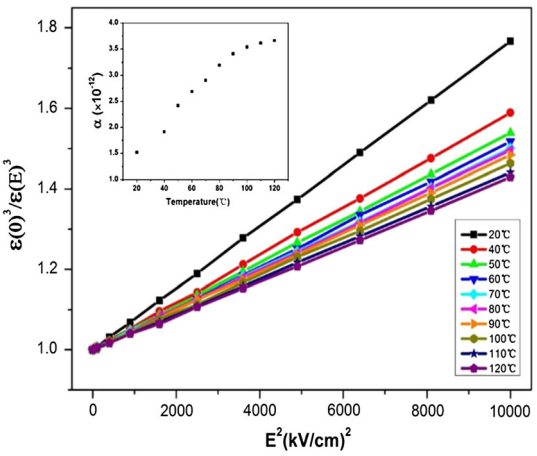

Figure 4 The $\varepsilon(0)^3/\varepsilon(E)^3$ dependence on E^2 and anharmonic constant α at different temperatures.

vibration enhanced with increasing temperature. Therefore, the permittivity–temperature (Fig. 3) and Devonshire phenomenological theory both explain the relationship between rate of change in dielectric constant and temperature under external electric field.

In light of Fig. 5, the energy storage density of BSZT-118 increases as the electric field from 30 to 100 kV/cm, but it decreases with the test temperature increasing. The tunability of energy storage density of BSZT-118 increases with increasing the electric field (see the change trend of the same color points in Fig. 5). Simultaneously, according to the formula [24, 25]:

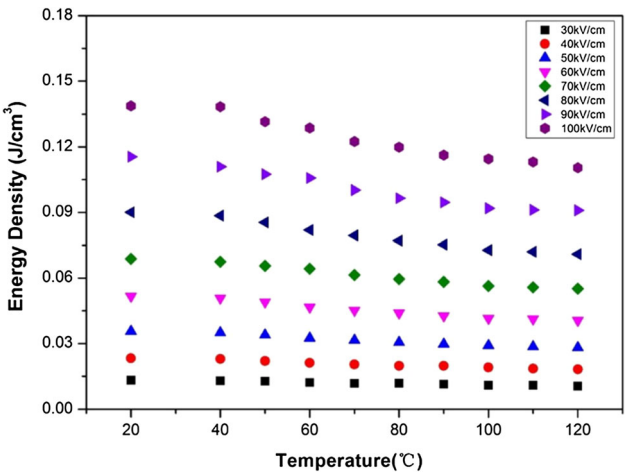

Figure 5 The impact of electric field on energy density at different test temperatures.

$$W = \int_{P_r}^{P_{max}} EdP \tag{5}$$

where P_{max} and P_r are the maximum polarization and remanent polarization, respectively. P is the polarization; E is the applied electric field. The energy storage density (W) increases with the increase in electric field (E), but the permittivity (ε) would decrease when temperature or electric field increases, so it is difficult to determine that the energy storage density increases or not due to improving electric field when the temperature is different. As shown in Fig. 5, the energy storage density at 20 °C and 90 kV/cm is larger than energy density at 120 °C and 100 kV/cm; this means that the permittivity because of impact of electric field and temperature is more influential than electric field on energy density in the situation. However, it also proves that α increases as test temperature rises and the application conditions are very important for the energy storage density.

In order to further illustrate the energy storage density under external electric field, it is important to focus on the impact of test temperature on the energy density at different electric fields. The energy density stability of the BSZT-118 against electric field at different temperatures is defined as:

$$R = \frac{W_{20} - W_T}{W_{20}} \tag{6}$$

where W_{20} and W_T are the energy density of 20 °C and different test temperatures (70–120 °C) at different electric fields, respectively. In Fig. 6, the result shows that the value of R increases with temperature increasing, which means the energy density stability decreases as the temperature increases. Besides, this value is minimum when the electric field is 70 kV/cm from 70 to 120 °C that explains the dielectric properties of BSZT-118 are the most stable at 70 kV/cm from 70 to 120 °C.

Furthermore, the relationship between electric field and temperature on energy efficiency (η) has studied. Based on the following formula [26]:

$$\eta = \frac{\int_{P_r}^{P_{max}} EdP}{\int_{P_r}^{P_{max}} Edp} \times 100\% \tag{7}$$

We got Tables 1 and 2. As shown in Table 1, the energy efficiency of different temperatures is different under the electric field of 100 kv/cm, and the energy efficiency shows a downward trend with the increase in temperature, which is related to the increase in loss energy with the rising temperature. Furthermore, the discharge efficiency is little affected by temperature, below 100 °C. However, in light of Table 2, at 120 °C, the energy efficiency of BSZT is different under different electric fields and there is no obvious law. And the energy efficiency differs very little under different electric fields. Therefore, the energy efficiency shows a downward trend with the increase in temperature, but has little connection with the electric field.

The leakage current limiting the charge retention and influencing the ferroelectric hysteresis loop is an important characteristic of pulsed power capacitors [27]. There are many conduction mechanisms of

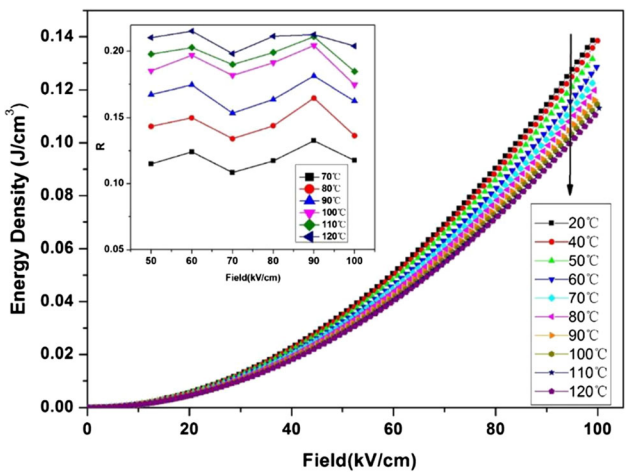

Figure 6 The impact of test temperature on the energy density at different electric fields.

Table 1 The energy efficiency of BSZT-118 at different temperatures at 100 kv/cm (T represents temperature)

T (°C)	20	40	50	60	70
η (%)	99.46	99.80	99.92	99.68	99.41
T (°C)	80	90	100	110	120
η (%)	99.21	98.81	96.41	95.75	92.68

Table 2 The energy efficiency of BSZT-118 with different electric fields at 120 °C

E (kV/cm)	30	40	50	60
η (%)	93.45	91.37	92.50	90.98
E (kV/cm)	70	80	90	100
η (%)	92.35	90.54	90.16	92.68

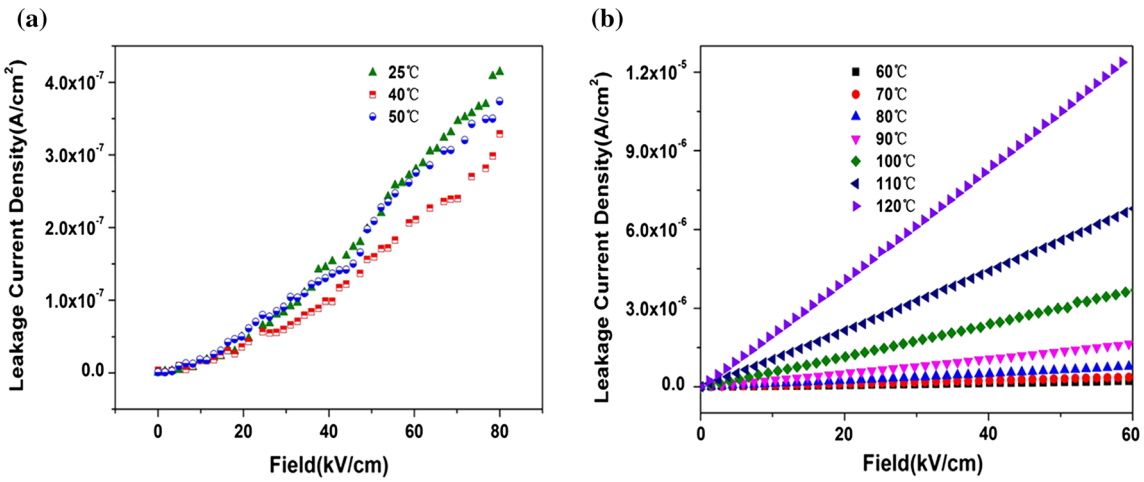

Figure 7 The leakage current density of BSZT-118 at different test temperatures (**a**, **b**).

dielectric material. For the ohmic conduction in a plane parallel platter of thickness (t), the current density (J) is defined as [28, 29]

$$J = en\mu\frac{V}{t} \tag{8}$$

where e is the electronic charge, n is the free charge carrier density, and μ and V are the charge carrier mobility and the voltage applied to the electrodes of the sample, respectively. The J is directly proportional to the V, so the J–E curve is linear for the same sample. In the meanwhile, for the space charge-limited conduction (SCLC), the current density can be described based on [29]

$$J = \frac{9}{8}\theta\varepsilon\mu\frac{V^2}{t^3} \tag{9}$$

where θ is the ratio of the free charge carrier concentration and ε is the permittivity. Therefore, the J–E characteristic of SCLC is characterized by nonlinearity. In Fig. 7, the leakage current with electric field shows the different conduction mechanisms at different temperatures. Below 60 °C, the leakage current is nonlinear with the electric field, consistent with the J–V curve characteristics of the space charge-limited conduction (SCLC) [28], as shown in Fig. 7a. However, in Fig. 7b, the leakage current with electric field shows the Ohm's law and increases when the temperature rises [30]. This shows that the leakage conduction mechanism of BSZT-118 below 60 °C is dominated by SCLC, and above 60 °C is the Ohm's law.

Conclusions

The dielectric properties and energy storage density of BSZT-118 are affected by temperature and electric field. Nonlinear dielectric behavior of BSZT-118 under high electric field is mainly caused by anharmonic interaction between Ti ion and Zr ion, which is accorded with Johnson's formula. Furthermore, it can give a quantitative explanation to its dielectric nonlinearity and the anharmonic constant α increases with increasing temperature.

Temperature stability of energy storage density decreases when the electric field increases, and the dielectric properties of BSZT-118 are the most stable at 70 kV/cm from 70 to 120 °C. The energy efficiency shows a downward trend with the increase in temperature, but has little connection with the electric field. The BSZT-118 has different conduction mechanisms at different temperatures, and the leakage conduction mechanism of BSZT-118 below 60 °C is dominated by SCLC, but above 60 °C is the Ohm's law.

Acknowledgements

This work is supported by the National Natural Science Foundation of China under Grant No. u1601208.

Compliance with ethical standards

Conflict of interest The manuscript is approved by all authors for publication and there is no conflict of interest exits in the submission of this manuscript.

References

[1] Hu Q, Wang T, Jin L et al (2014) Dielectric and energy storage properties of barium strontium titanate based glass–ceramics prepared by sol–gel method. J Sol–Gel Sci Technol 71(3):522–529

[2] Jo HR, Lynch CS (2016) A high energy density relaxor antiferroelectric pulsed capacitor dielectric. J Appl Phys 119(2):024104

[3] Wisken HG, Podeyn F, Weise HGG (2001) High energy density capacitors for ETC gun applications. IEEE Trans Magn 37(1):332–335

[4] MacDougall FW, Ennis JB, Cooper RA et al (2003) High energy density pulsed power capacitors. In: IEEE international pulsed power conference, vol 1, pp 513–517

[5] Dai L, Lin F, Zhu Z et al (2005) Electrical characteristics of high energy density multilayer ceramic capacitor for pulse power application. IEEE Trans Magn 41(1):281–284

[6] Gorzkowski EP, Pan MJ, Bender B et al (2007) Glass-ceramics of barium strontium titanate for high energy density capacitors. J Electroceram 18(3–4):269–276

[7] Yang H, Liu P, Yan F et al (2019) A novel lead-free ceramic with layered structure for high energy storage applications. J Alloy Compd 773:244–249

[8] Feng L, Mingxing Z, Jiwei Z et al (2018) Novel barium titanate based ferroelectric relaxor ceramics with superior charge-discharge performance. J Eur Ceram Soc 38:4646–4652

[9] Feng L, Tao J, Jiwei Z et al (2018) Exploring novel bismuth-based material for energy storage applications. J Mater Chem C 6:7976–7981

[10] Hilton AD, Ricketts BW (1996) Dielectric properties of ceramics. J Phys D Appl Phys 29(5):1321–1325

[11] Kumar M, Garg A, Kumar R et al (2008) Structural, dielectric and ferroelectric study of $Ba_{0.9}Sr_{0.1}Zr_xTi_{1-x}O_3$ ceramics prepared by the sol–gel method. Phys B Condens Matter 403(s10–11):1819–1823

[12] Ricketts BW, Triani G, Hilton AD (2000) Dielectric energy storage densities in $Ba_{1-x}Sr_xTi_{1-y}Zr_yO_3$ ceramics. J Mater Sci: Mater Electron 11(6):513–517

[13] Xu Q, Zhan D, Huang DP et al (2013) Effect of MgO–CaO–Al_2O_3–SiO_2 glass additive on dielectric properties of $Ba_{0.95}Sr_{0.05}Zr_{0.2}Ti_{0.8}O_3$ ceramics. J Alloy Compd 558:77–83

[14] Tang XG, Wang XX, Chew KH et al (2005) Relaxor behavior of (Ba, Sr)(Zr, Ti)O3 ferroelectric ceramics. Solid State Commun 136(2):89–93

[15] Mangaiyarkkarasi J, Sasikumar S, Saravanan OV et al (2017) Electronic structure and bonding interactions in $Ba_{1-x}Sr_xZr_{0.1}Ti_{0.9}O_3$ ceramics. Front Mater Sci 11(2):182–189

[16] Jian X, Lu B, Li D et al (2019) Enhanced electrocaloric effect in Sr^{2+}-modified lead-free $BaZr_xTi_{1-x}O_3$ ceramics. ACS Appl Mater Interfaces 11(22):20167–20173

[17] Alexandru HV, Berbecaru C, Ioachim A et al (2006) BST solid solutions, temperature evolution of the ferroelectric transitions. Appl Surf Sci 253(1):354–357

[18] Ho IC, Fu SL (1990) Effects of zirconium on the structural and dielectric properties of (Ba, Sr) TiO_3 solid solution. J Mater Sci 25(11):4699–4703. https://doi.org/10.1007/BF01129927

[19] Johnson KM (1962) Variation of dielectric constant with voltage in ferroelectrics and its application to parametric devices. J Appl Phys 33(9):2826–2831

[20] Placeres-Jiménez R, Rino JP, Eiras JA (2015) Modeling ferroelectric permittivity dependence on electric field and estimation of the intrinsic and extrinsic contributions. J Phys D Appl Phys 48(3):035304

[21] Ang C, Yu Z (1970) DC electric-field dependence of the dielectric constant in polar dielectrics: multipolarization mechanism mode l. Phys Rev B Condens Matter 69(17):1324–1332

[22] Diamond H (1961) Variation of permittivity with electric field in perovskite-like ferroelectrics. J Appl Phys 32(5):909–915

[23] Outzourhit A, Trefny JU, Kito T et al (1995) Tunability of the dielectric constant of $Ba_{0.1}Sr_{0.9}TiO_3$ ceramics in the paraelectric state. J Mater Res 10(06):1411–1417

[24] Li W, Zhou D, Pang L (2017) Enhanced energy storage density by inducing defect dipoles in lead free relaxor ferroelectric $BaTiO_3$-based ceramics. Appl Phys Lett 110:132902

[25] Yang H, Yan F, Lin Y, Wang T (2017) Novel strontium titanate-based lead-free ceramics for high energy storage applications. ACS Sustain Chem Eng 5:10215–10222

[26] Wang T, Wang YH, Yang HB et al (2018) Structure, dielectric properties of low temperature-sintering BaTiO3-based glass-ceramics for energy storage. J Adv Dielect 08(06):1850041

[27] Reshmi R, Asha AS, Krishnaprasad PS et al (2011) High tunability of pulsed laser deposited $Ba_{0.7}Sr_{0.3}TiO_3$ thin films

on perovskite oxide electrode. J Alloy Compd 509(23):6561–6566

[28] Neusel C, Jelitto H, Schneider GA (2015) Electrical conduction mechanism in bulk ceramic insulators at high voltages until dielectric breakdown. J Appl Phys 117(15):154902

[29] Kao KC (2004) Dielectric phenomena in solids. Dielectric phenomena in solids

[30] Li R, Jiang S, Gao L et al (2012) Enhanced leakage current performance and conduction mechanisms of $Bi_{1.5}Zn_{1.0}Nb_{1.5}O_7/Ba_{0.5}Sr_{0.5}TiO_3$ bilayered thin films. J Appl Phys 112(7):074113